Ryan Ochoa

10/08/21

Nociceptors and TRP Channels

Luna was sleeping on the floor on the blanket & rose just dragged the blanket, took it and put it on the bed

Background - Nociceptors

- Specialized sensory neurons

  - DRG (or other primary sensory neurons)

  - Afferent and efferent function

    - A: L-glutamate

    - E: Substance P and CGRP

- Found skin, muscle, joints and viscera

- Detect noxious or damaging stimuli

  - Sensitization – GPCR and Tyrosine kinase receptor

Background - Nociceptors

Two Groups of Nociceptors:

1. Medium diameter myelinated

2. Small diameter unmyelinated

Background - Nociceptors

Medium diameter myelinated (Aδ)

- Acute and fast pain

- Two subtypes:

  - Type I

    - Mechanical and chemical

    - High heat threshold (>50 C)

  - Type II

    - Very high mechanical threshold
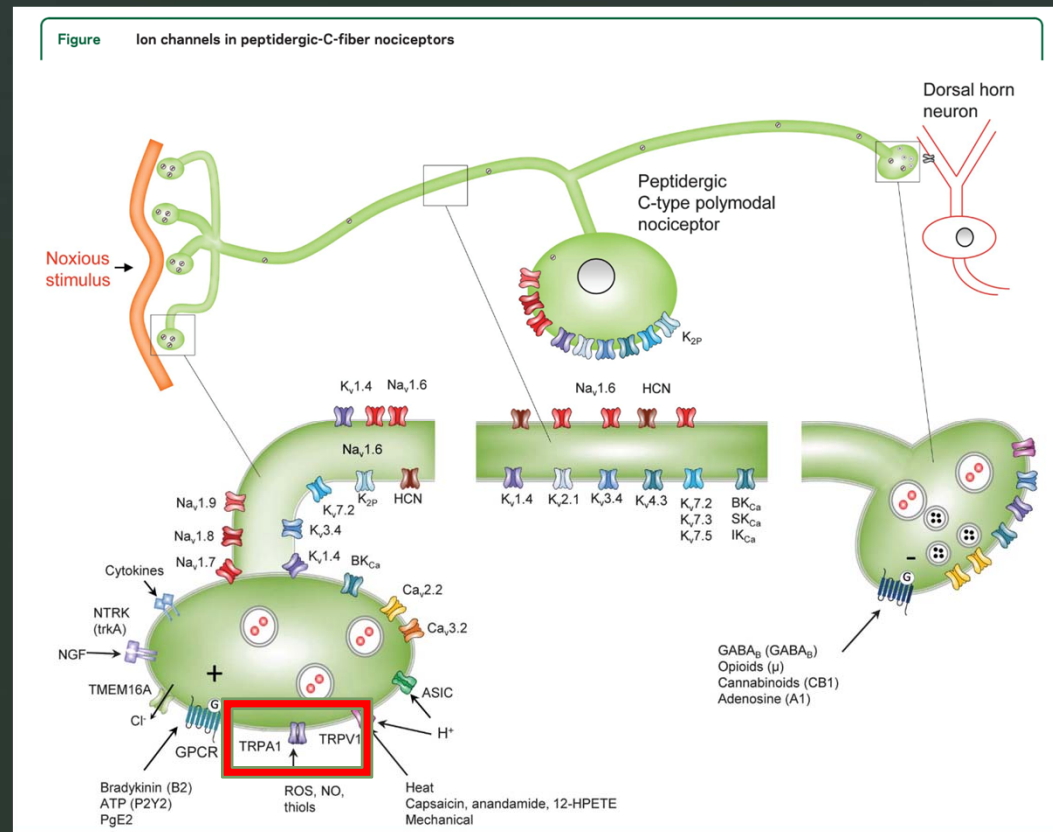
    - Low heat threshold

Background - Nociceptors

Small diameter unmyelinated (C)

- Slow and "second"

- Mechanical and heat sensitive

  - Ex. Heat sensitive, or mechano-cold sensitive

Background - Nociceptors

Figure   Ion channels in peptidergic-C-fiber nociceptors

Background - Nociceptors

Channel	Function	Comments (including findings in experimental models)
Na$_v$1.7	Threshold channel; large ramp current that amplifies subthreshold stimuli	Also expressed in sympathetic ganglia and olfactory neurons; upregulated in the setting of inflammation and nerve injury
Na$_v$1.8	Most of the current underlying the action potential; supports repetitive action potential firing	Upregulated by NGF in the setting of accumulation at site of axonal injury
Na$_v$1.9	Slow activation at voltage close to the RMP and ultraslow inactivation; amplifies and prolongs small subthreshold depolarizations and depolarizes the RMP	Downregulated in axonal injury; activated in response to inflammatory mediators
K$_v$1.1	Mediates slowly inactivating, delayed-rectifier currents responsible for action potential repolarization	Downregulated in axon injury; forms a complex with CASPR2 that is target of autoantibodies
K$_v$2.2	Influences membrane repolarization and interspike hyperpolarization during repetitive firing	Downregulated after nerve or oxaliplatin-induced injury
K$_v$3.4	Rapidly inactivating current that accelerates repolarization and may restrict Ca^{2+}-dependent neurotransmitter release	Downregulated in axon injury and diabetic neuropathy
K$_v$4.3, K$_v$1.4	Fast activation and inactivation; mediate A-type currents that limit action potential threshold, duration, and firing frequency	Downregulated in the setting of injury via REST
K$_v$7 (K$_v$7.2, K$_v$7.3, and K$_v$7.5)	Open near RMP and mediate a low-threshold noninactivating M current that stabilizes the RMP and regulates action potential threshold and accommodation	Downregulated in the setting of injury via REST; activated by retigabine and flupirtine
K$_{Ca}$	Activated by Ca2$^+$ accumulated during neuronal firing; provides a feedback inhibition that slows repetitive action potential firing; BK$_{Ca}$ is functionally coupled to TRPV1	Reduced expression after axotomy; inhibited by PGE2 and other inflammatory mediators
K$_{Na}$	Na$^+$-activated K$^+$ channel that contributes to a long-lasting slow hyperpolarization that follows repetitive firing	Downregulated by internalization during inflammation
K$_2$P	Constitutively open; generates background "leak" current that stabilizes the RMP below firing threshold	TRESK downregulated in axon injury; TASK downregulated during inflammation
Ca$_v$1.2 (L)	May contribute to nociceptor excitability and peripheral release of neuropeptides	Upregulated after axotomy; mediates neuropathic pain
Ca$_v$2.2 (N)	Located in presynaptic terminals and triggers release of glutamate, substance P, and CGRP both at central and peripheral terminals of nociceptors	The $\alpha 2\delta$ subunit increases membrane expression of the $\alpha 1$ subunit, is upregulated in inflammatory and neuropathic pain, and is the target of gabapentin and pregabalin
Ca$_v$3.2 (T)	Promotes burst firing; may promote glutamate release from nociceptive terminals in the dorsal horn	May contribute to central mechanisms of pain
TRPV1	Activated by noxious heat, low pH, capsaicin, and bioactive lipids such as anandamide; critically involved in heat-induced pain and acid-evoked sensitization	Target on multiple inflammatory mediators triggering nociceptor sensitization
TRPA1	Molecular integrator of many exogenous and endogenous noxious stimuli, including oxygen and nitrogen free radicals	Coexpressed with TRPV1 in a subset of peptidergic nociceptors; upregulated during inflammation
TRPM8	Activated by both innocuous and noxious cold	Contributes to cold allodynia in the setting of oxaliplatin-induced and other neuropathies
ASIC	Activated by acidic pH; permeable to Na$^+$ and elicits cell depolarization	ASIC3 is pH sensor for muscle pain triggered by lactic acid
HCN	Activated by hyperpolarization; permeable to Na$^+$ and K$^+$ and constitutively open near RMP; positively modulated by cAMP	HCN2 has a role in inflammatory and neuropathic pain; HCN1 may contribute to cold hyperalgesia and allodynia in oxaliplatin-induced neuropathy
TMEM16A (ANO1)	Ca^{2+}-activated Cl− channel; elicits Cl− efflux resulting in membrane depolarization and triggering of action potentials	Activated by bradykinin and heat
P2X$_3$	Activated by ATP; permeable to Na$^+$, K$^+$, and Ca^{2+}	Mediates mechanosensory transduction in viscera and participates in somatic and visceral pain
5-HT$_3$R	Activated by serotonin, permeable to Na$^+$ and Ca^{2+}	Contributes to persistent nociceptive processing in the setting of injury
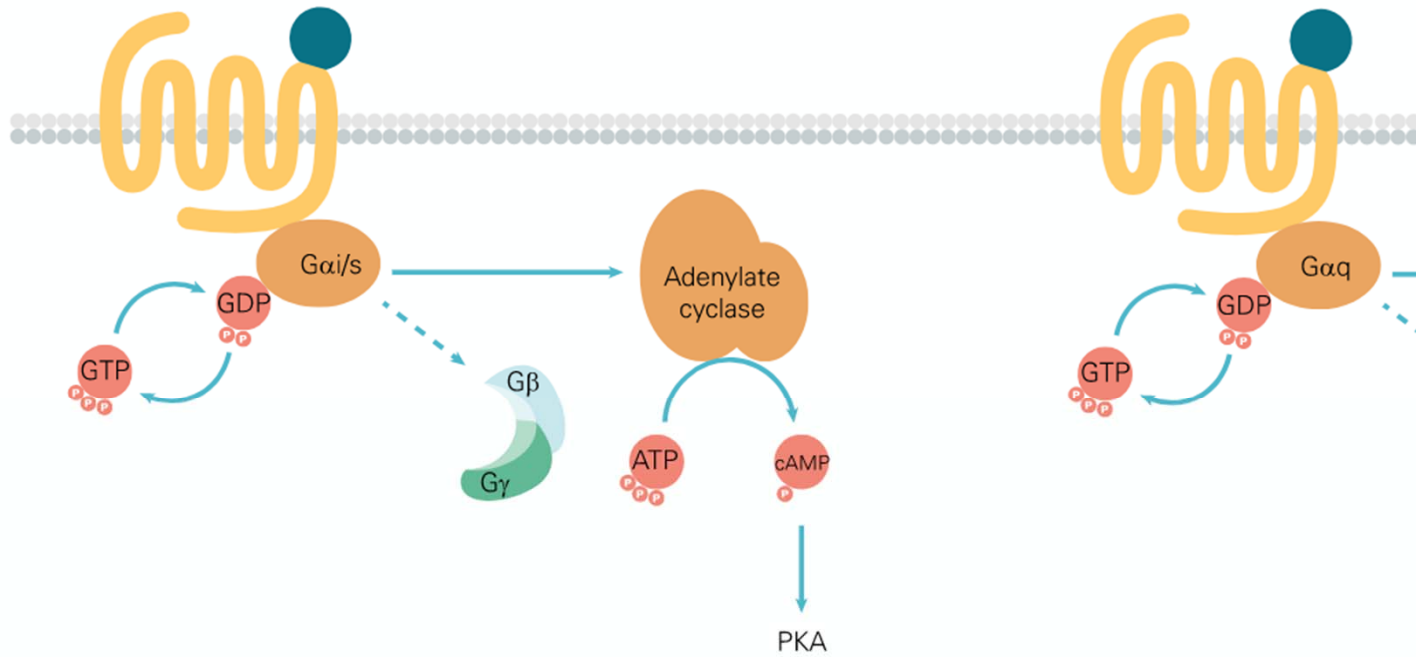
Nociceptors/TRPs – Importance?

- Paroxysmal extreme pain disorders

  - Rectal, perineal, ocular and mandibular pain

  - Sodium channel ($Na_V1.7$) gain of function mutation

- Familial episodic pain disorder

  - TRPA1 mutation

  - Severe episodic pain

    - Thorax and arms

    - Sweating, generalized pallor, periubuccal cyanosis, tachycardia, breathing difficulties and abdominal wall stiffness

More recently, clinical studies integrating phenotypic characterization, genetics, and in vitro elucidation of the functional effects of **mutations have clearly established that Na$_v$ (and TRPA1) nociceptor channelopathies are an important cause of episodic pain disorders, insensitivity to pain, and painful SFN**. Some evidence indicates that auto-immune K$_v$ channelopathies may at least contribute to otherwise unexplained pain.

Nobel Prize 2021

David Julius and Ardem Patapoutian

Nobel Prize 2021

David Julius

- Used capsaicin to show how we interpret "heat" as chemical signals

- Had a library of millions of DNA fragments – only one single gene was coded for heat

- Discovered TRPV1 – activates at temperatures deemed as painful

https://www.nobelprize.org/prizes/medicine/2021/press-release/

Nobel Prize 2021

Ardem Patapoutian

- Found a cell line that generated signals due to being probed with a micropipette

- Inactivated gene after gene until..

- Discovery of Piezo1! (Greek for pressure)

- Ion channels directly activated by exertion of pressure on membrane

- Important for proprioception but regulate blood pressure, respiration and urinary bladder control

https://www.nobelprize.org/prizes/medicine/2021/press-release/

Takaharu Okada‡, Shunichi Shimizu‡, Minoru Wakamori‡, Akito Maeda¶, Tomohiro Kurosaki¶,Naoyuki Takada‡§, Keiji Imoto‡, and Yasuo Mori‡§

Molecular Cloning and Functional Characterization of a NovelReceptor-activated TRP Ca21Channel from Mouse Brain

Calcium

- Important in regulation

- Can be released intracellularly by IP_3

- Connection between Ca^{2+} and TRP5?

A

```
MAQLYYKKVNYSPYRDRIPLQIVRAETELSAEEKAFLSAVEKGDYATVKQALQEAEIYYN        1 - 60
VNINCMDPLGRSALLIAIENENLEIMELLNHSVYVGDALLYAIRKEVVGAVELLLSYRK        61 - 120
PSGEKQVPTLMMDTQFSEFTPDITPIMLAAHTNNYEIIKLLVQKRVTIPRPHQIRCNCVE      121 - 180
CVSSSEVDSLRHSRSRLNIYKALASPSLIALSSEDPILTAFRLGWELKELSKVENEFKAE      181 - 240
YEELSQQCKLFAKDLLDQARSSRELEIILNHRDDHSEELDPQKYHDLAKLKVAIKYHQKE      241 - 300
FVVQPNCQQLLATLWYDGFPGWRRKHWVVKLLTCMTIGFLFPMLSIAYLISPRSNLGLFI    301 - 360
                                  H1
KKPFIKFICHTASYLTFLFMLLLASQHIVRTDLHVQGPPPTVVEWMILPWVLGFIWGEIK    361 - 420
   H2                                        H3
EMWDGGFTEYIHDWWNLMDFAMNSLYLATISLKIVAYVKYNGSRPREEWEMWHPTLIAEA    421 - 480
               H4
LFAISNILSSLRLISLFTANSHLGPLQISLGRMLLDILKFLFIYCLVLLAFANGLNQLYF    481 - 540
H5                          H6
YYETRAIDEPNNCKGIRCEKQNNAFSTLFETLQSLFWSVFGLLNLYVTNVKARHEFTEFV    541 - 600
                           H7
GATMFGTYNVISLVVLLNMLIAMMNNSYQLIADHADIEWKFARTKLWMSYFDEGGTLPPP    601 - 660
H8
FNIIPSPKSFLYLGNWFNNTFCPKRDPDGRRRRHNLRSETERHADSLIQNQHYQEVIRNL    661 - 720
VKRYVAAMIRNSKTNEGLTEENFKELKQDISSFRYEVLDLLGNRKHPRRSLSTSSADFSQ    721 - 780
RDDTNDGSGGARAKSKSVSFNVGCKKKACHGAPLIRTVPRASGACQKPKSESSSKRSFMG    781 - 840
PSFKKLGLFFSKFNGQTSEPTSEPMYTISDGIAQQHCMWQDIRYSQMEKGKAEACSQSQM    841 - 900
NLGEVELGEIRGAAARSSECPLACSSSLHCASGICSSNSKLLDSSEDVFETWGEACDLLM    901 - 960
HKWGDGQEEQVTTRL                                                 961 - 975
```
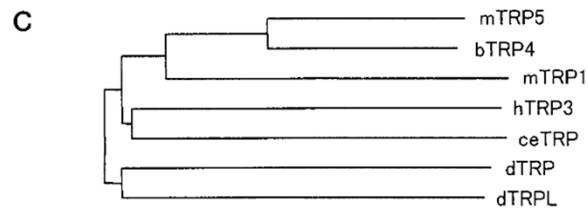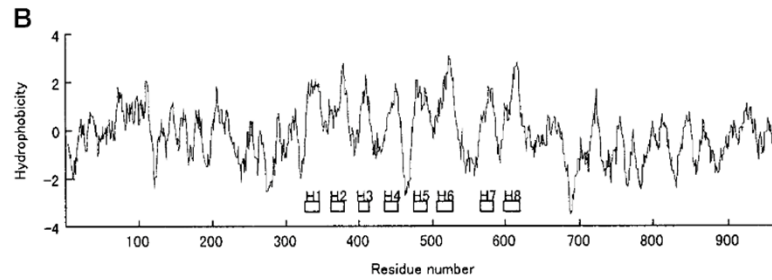
B

C

FIG. 1. **Primary structure and hydropathy analysis of TRP5, and phylogenetic tree of the TRP family.** In A, the amino acid sequence (in *single-letter code*) of the mouse brain TRP5 deduced from the cDNA sequence is shown. The hydrophobic regions H1–H8 are enclosed with *solid lines*. The domains predicted to form coiled-coil structure are *underlined* with *dashed lines*. In B, the Kyte-Doolittle hydrophobicity profile of TRP5 was generated with a window size of 10 amino acids (66). In C, the phylogenetic tree for the TRP family was generated using the Clustalw program (46). Members of the TRP family are as follows: dTRP (42), dTRPL (43), hTRP3 (24), bTRP4 (25), ceTRP (67), and mTRP1 (68).

A

forebrain, hindbrain, skeletal muscle, heart, lung, liver, spleen, kidney, testis, uterus

9.5 —
7.5 —
4.4 —
2.4 —
1.4 —

B

forebrain, hindbrain, skeletal muscle, heart, lung, liver, spleen, kidney, testis, uterus

400 —
300 —
200 —

TRP5

cyclophilin

FIG. 2. **Distribution of TRP5 mRNA expression in the mouse tissues.** *A*, autoradiogram of blot hybridization analysis with a TRP5 cDNA probe of RNA from different tissues of mice. The positions and sizes (in kb) of the RNA markers are shown on the *left*. *B*, autoradiogram of blot hybridization analyses of TRP5 and cyclophilin cDNA fragments amplified by RT-PCR. Probes are 5′-end-labeled oligonucleotides internal to the primers used for PCR. The positions and sizes (in base pairs) of DNA markers are shown on the *left*.
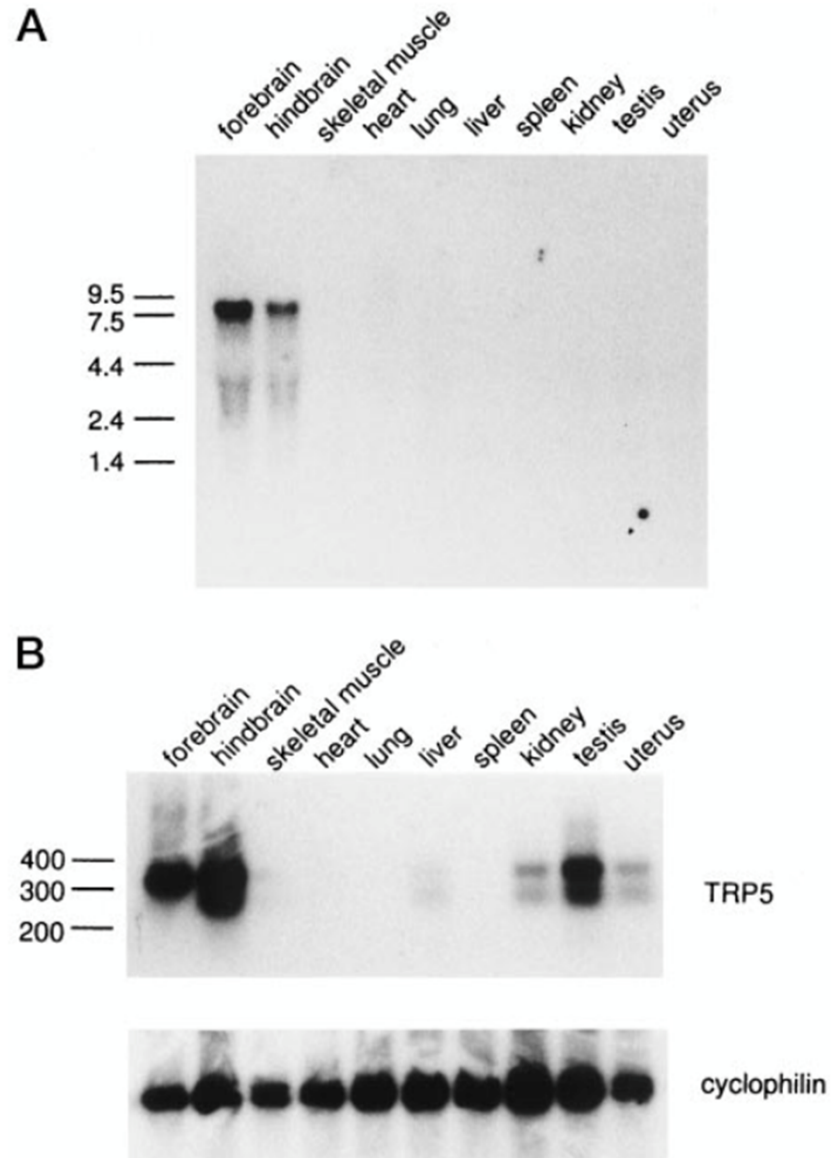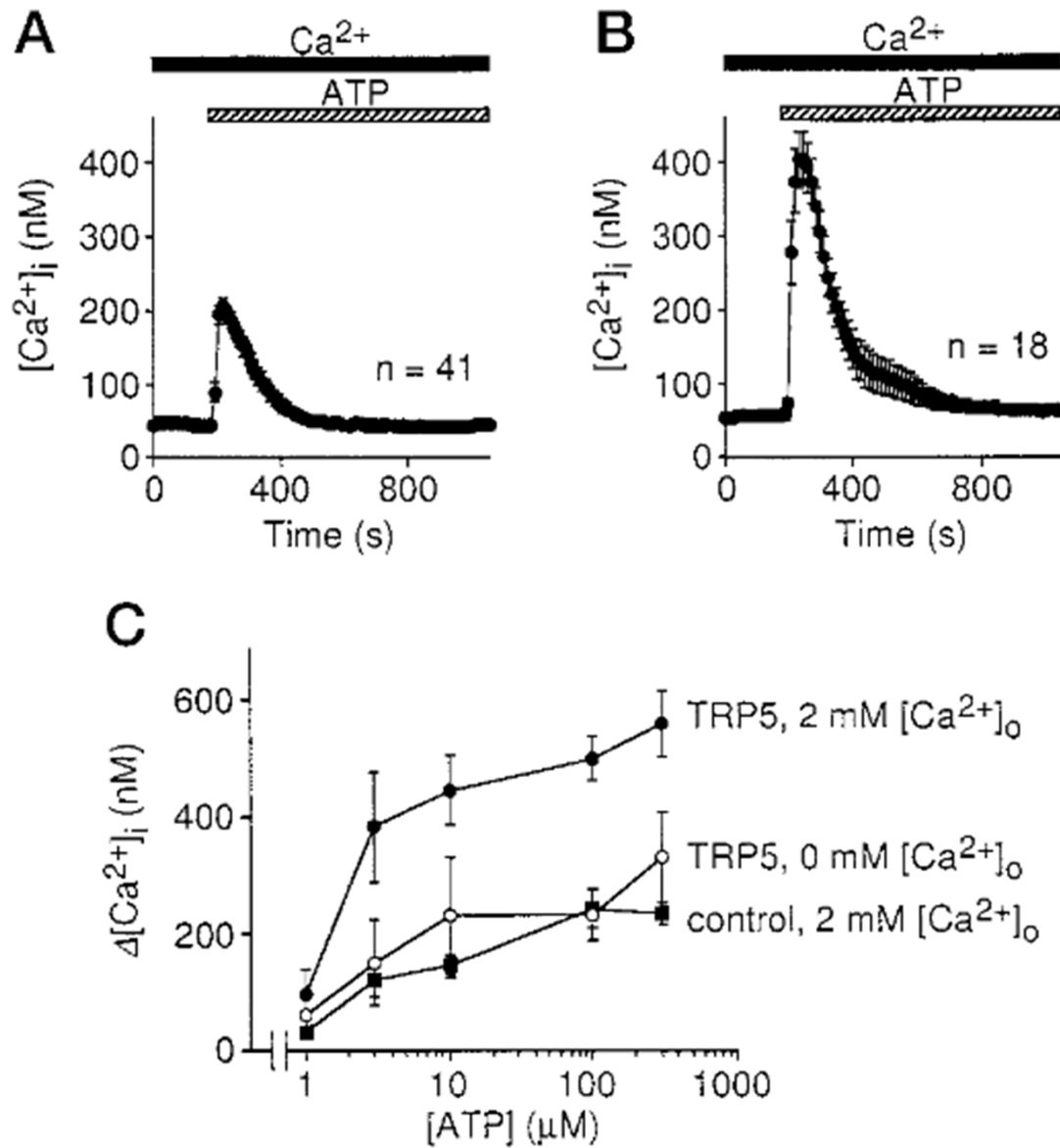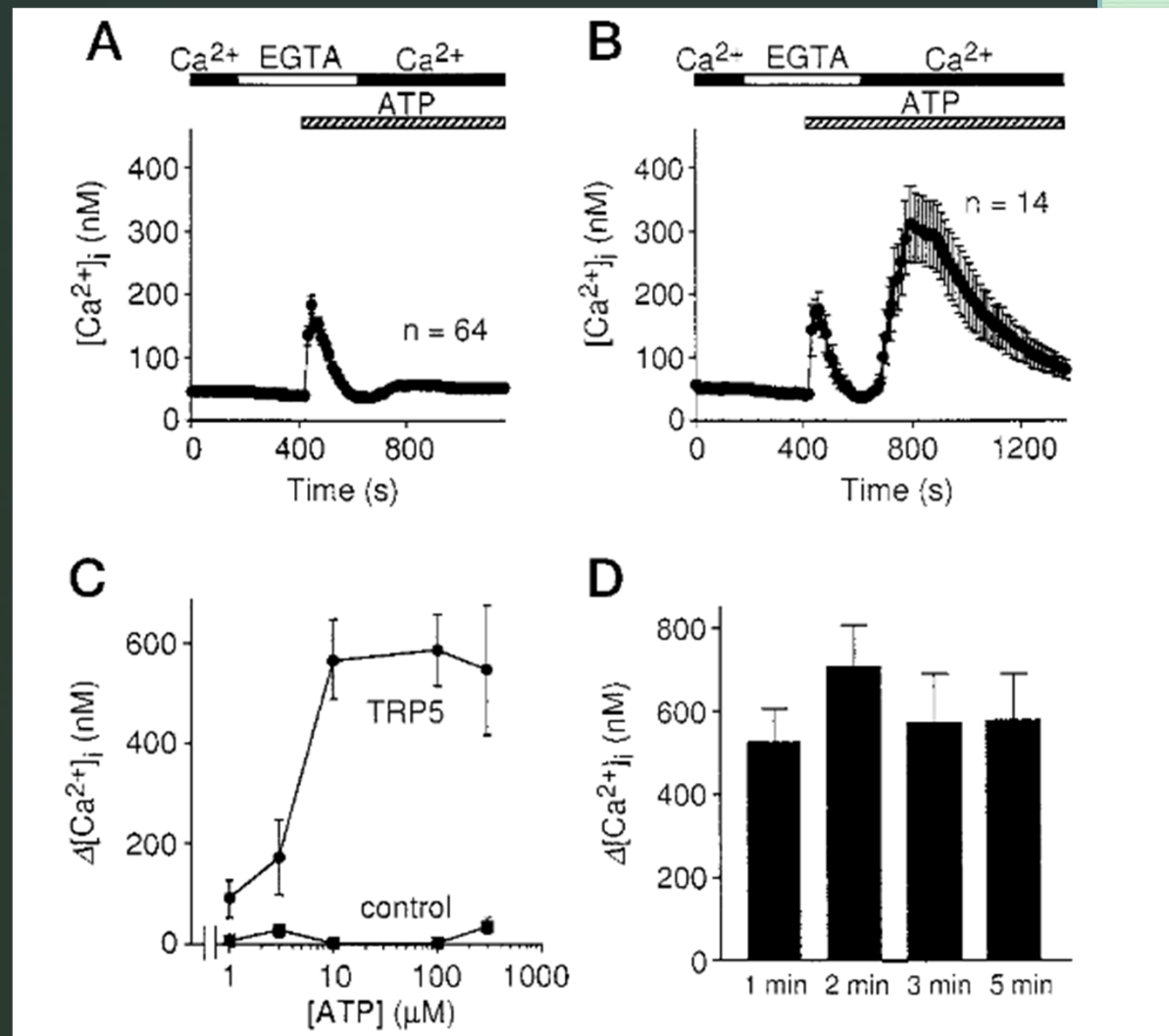
FIG. 3. **ATP-induced $[Ca^{2+}]_i$ transients in control and TRP5-transfected HEK cells in the presence of extracellular Ca^{2+}.** Cytosolic Ca^{2+} was measured in fura-2-loaded control HEK293 cells (*A*) or HEK293 cells transfected with TRP5 plus CD8 (*B*). The cells were treated with 100 μM ATP in the presence of 2 mM extracellular Ca^{2+}. The duration of exposure to Ca^{2+}-containing HBS and 100 μM ATP is indicated by the *filled* and *hatched bars*, respectively, above the graphs. *C*, dose-response relationships for maximum ATP-induced $[Ca^{2+}]_i$ rises ($\Delta[Ca^{2+}]_i$) in individual control HEK293 cells (*filled box*) or HEK293 cells transfected with TRP5 plus CD8 cDNAs (*filled circle*) in the presence of 2 mM extracellular Ca^{2+}, and in TRP5-transfected cells in the absence of extracellular Ca^{2+} (*open circle*). Data points are the means ± S.E. $[Ca^{2+}]_i$ (*A* and *B*) or the means ± S.E. $\Delta[Ca^{2+}]_i$ (*C*) in 30–41 control HEK cells or 14–20 TRP5-transfected cells.

FIG. 4. **Separation of ATP-induced $[Ca^{2+}]_i$ transients due to Ca^{2+} release from internal stores and Ca^{2+} influx in TRP5-transfected HEK cells.** Cytosolic Ca^{2+} was measured in fura-2-loaded control HEK293 cells (*A*) or HEK293 cells transfected with TRP5 plus CD8 (*B*). In *A* and *B*, the perfusion solution was first changed to Ca^{2+}-free HBS containing 0.5 mM EGTA, and 100 μM ATP was applied to the cells in the absence of extracellular Ca^{2+}. Three min after the application of ATP, 2 mM Ca^{2+} was further added to the extracellular solution. The duration of exposure to Ca^{2+}-containing HBS, Ca^{2+}-free HBS, and 100 μM ATP is indicated by the *filled*, *open*, and *hatched bars*, respectively, above the graphs. *C*, concentration dependence of maximum $[Ca^{2+}]_i$ rises ($\Delta[Ca^{2+}]_i$) induced by the addition of 2 mM extracellular Ca^{2+} 3 min after the addition of ATP in individual control HEK293 cells (*filled box*) and HEK293 cells transfected with TRP5 plus CD8 (*filled circle*). *D*, $\Delta[Ca^{2+}]_i$ in TRP5-transfected cells are shown for various time intervals between the initiation of ATP (100 μM) application and the addition of 2 mM extracellular Ca^{2+}. Small $\Delta[Ca^{2+}]_i$ for 1 min resulted from $[Ca^{2+}]_i$, which was not yet reduced to the basal level before the addition of extracellular Ca^{2+}. Data points and columns are the means $\pm$ S.E. $[Ca^{2+}]_i$ or the means $\pm$ S.E. $\Delta[Ca^{2+}]_i$ in 29–64 control HEK cells or 14–16 TRP5-transfected cells.
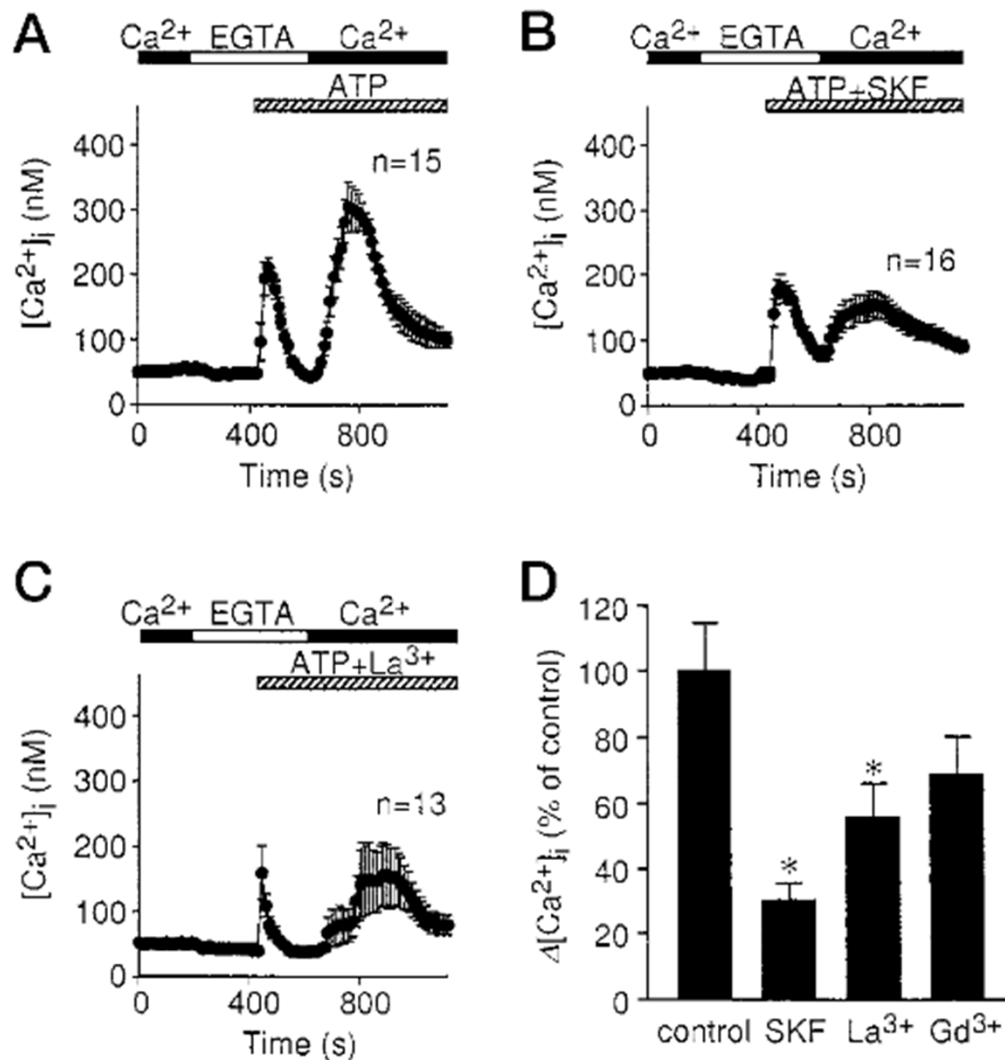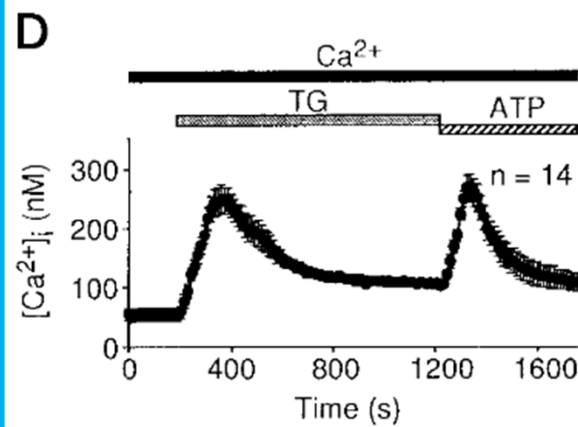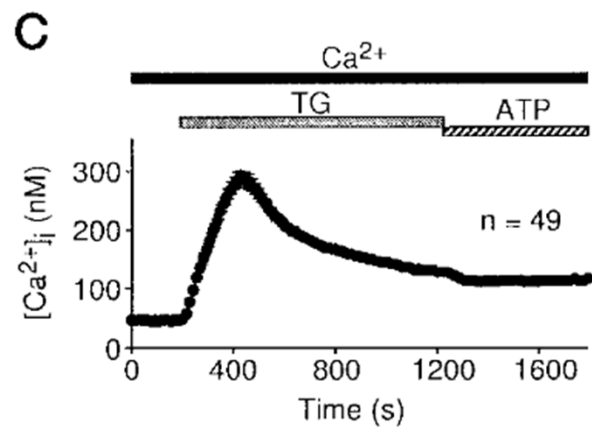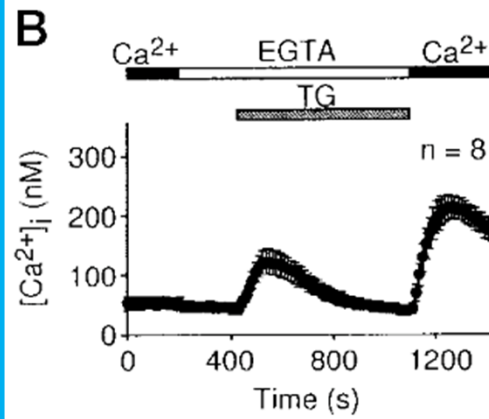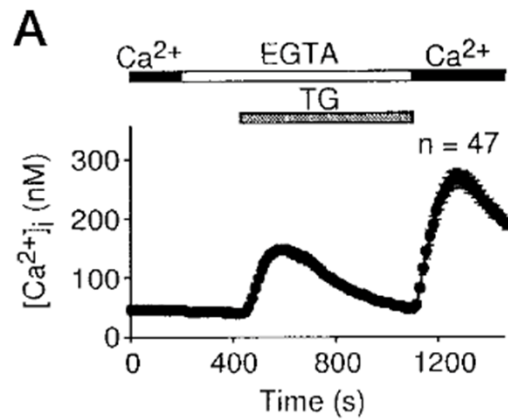
FIG. 5. **Pharmacological properties of ATP-induced Ca²⁺ influx in TRP5-transfected HEK cells.** Cytosolic Ca²⁺ was measured in fura-2-loaded TRP5-transfected cells. The perfusion solution was changed to Ca²⁺-free HBS, and 100 μM ATP alone (*A* and *D*), with 25 μM SK&F96365 (*B* and *D*), with 100 μM LaCl₃ (*C* and *D*), or with 100 μM GdCl₃ (*D*) was applied to the cells in the absence of extracellular Ca²⁺, which was followed by the addition of 2 mM extracellular Ca²⁺. The duration of exposure to Ca²⁺-containing HBS, Ca²⁺-free HBS, and 100 μM ATP alone or plus one of the drugs is indicated by the *filled*, *open*, and *hatched bars*, respectively, above the graphs. *D*, effects of 25 μM SK&F96365, 100 μM LaCl₃, and 100 μM GdCl₃ on the amplitude of maximum [Ca²⁺]ᵢ rises (Δ[Ca²⁺]ᵢ) induced by the addition of 2 mM extracellular Ca²⁺ 3 min after the addition of ATP in individual TRP5-transfected cells. For the experiments using lanthanides and their control experiments, KH₂PO₄ was omitted from HBS. The data shown in *A* are from the experiments using the phosphate-containing solution. S.E. from the experiments using the phosphate-free external solutions is shown for control Δ[Ca²⁺]ᵢ shown in *D*. Data points and columns are the means ± S.E. [Ca²⁺]ᵢ or the means ± S.E. Δ[Ca²⁺]ᵢ in 13–21 TRP5-transfected cells. Bonferroni's *t* test following analysis of variance was employed to determine the statistical significance of differences. *, $p < 0.05$, compared with the control.

FIG. 6. **Thapsigargin-induced $[Ca^{2+}]_i$ transients and ATP-induced $[Ca^{2+}]_i$ changes after store depletion in control and TRP5-transfected HEK cells.** Cytosolic Ca^{2+} was measured in fura-2-loaded control HEK293 cells (*A* and *C*) or HEK293 cells transfected with TRP5 plus CD8 (*B* and *D*). In *A* and *B*, the perfusion solution was changed to Ca^{2+}-free HBS containing 0.5 mM EGTA, and 2 μM thapsigargin (*TG*) was applied to the cells in the absence of extracellular Ca^{2+}, which was followed by the addition of 2 mM extracellular Ca^{2+}. In *C* and *D*, the cells were treated with 2 μM thapsigargin in the presence of extracellular Ca^{2+}, then thapsigargin was replaced with 100 μM ATP. The duration of exposure to Ca^{2+}-containing HBS, Ca^{2+}-free HBS, 100 μM ATP, and 2 μM thapsigargin is indicated by the *filled*, *open*, *hatched*, and *shaded* bars, respectively, above the graphs. Data points are the means ± S.E. $[Ca^{2+}]_i$ in the indicated number of cells.

■ Control HEK293 Cells

■ Experimental HEK293 Transfected Cells (w/ TRP5 and CD8)

FIG. 7. **Electrophysiological characterization of the TRP5 channel.** In *A*, shown is a time course of ionic current recorded from a control HEK293 cell at a holding potential of −50 mV. During application of ATP (indicated by the *hatched bar* above the current) to the control HEK293 cell, the external solutions were changed from the 0Ca²⁺ solution (*open bar*) to the 10Ca²⁺ solution (*filled bar*). Finally, ATP was washed out with the 0Ca²⁺ solution. In *B*, a time course of ionic current recorded from a HEK293 cell transfected with TRP5 plus CD8 is shown. In *C*, current-voltage relationships of the TRP5 channel are shown. Currents were evoked by 1.5-s negative voltage ramps from 40 to −70 mV. Five consecutive ramps were applied every 5 s in the 0Ca²⁺ solution or the 10Ca²⁺ solution with 100 μM ATP. The averaged currents were drawn. The currents shown in *B* and *C* were recorded from different TRP5-transfected cells.
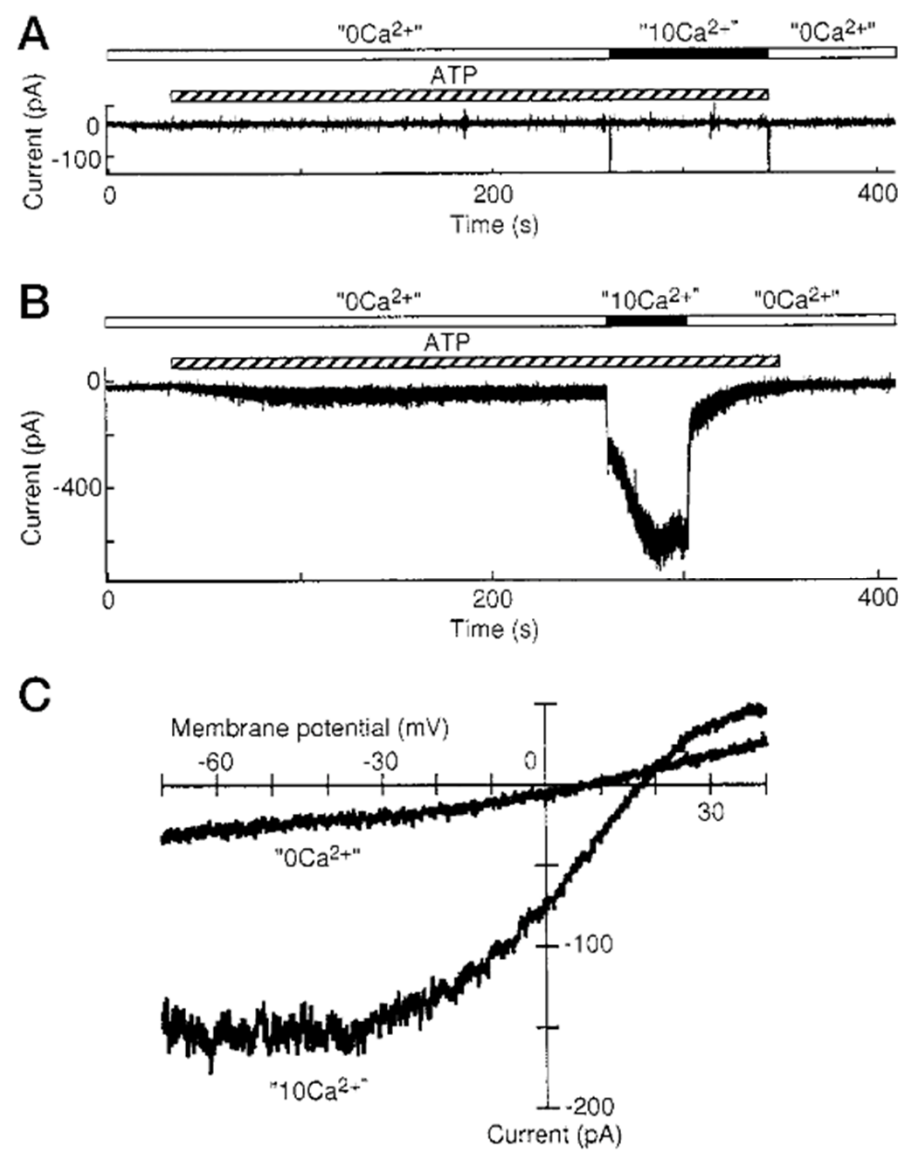
Conclusions

- Increases in intracellular calcium concentration linked to ATP in presence of extracellular calcium

- TRP5 permeable to calcium>monovalent ions

- Suggested there are other activators of TRP5

Kseniia Koroleva1,2*, Elizaveta Ermakova1, Alsu
Mustafina1, Raisa Giniatullina2,Rashid
Giniatullin1,2and Guzel Sitdikova1

Protective Effects of HydrogenSulfide Against the ATP-InducedMeningeal Nociception

Hydrogen Sulfide

- Common gaseous transmitter with many physiological roles

- Migraine pain associated with neuropeptides such as Calcitonin gene-related peptide (CGRP) and nitric oxide (NO) – induce pain

  - Less interest in pain-reducers

- Suggested as a transmitter in nociception

  - Contradictory evidence

Hydrogen Sulfide - Migraines

Pro-nociception

- Activates TRPV1 and TRPA1 receptors

Anti-nociception

- Activates ATP and calcium dependent potassium channels

- Antioxidant and anti-inflammatory

P2X Receptors

- Shown to be pro-nociception

- Mediated by ATP

- Expressed in 80% of trigeminal neurons

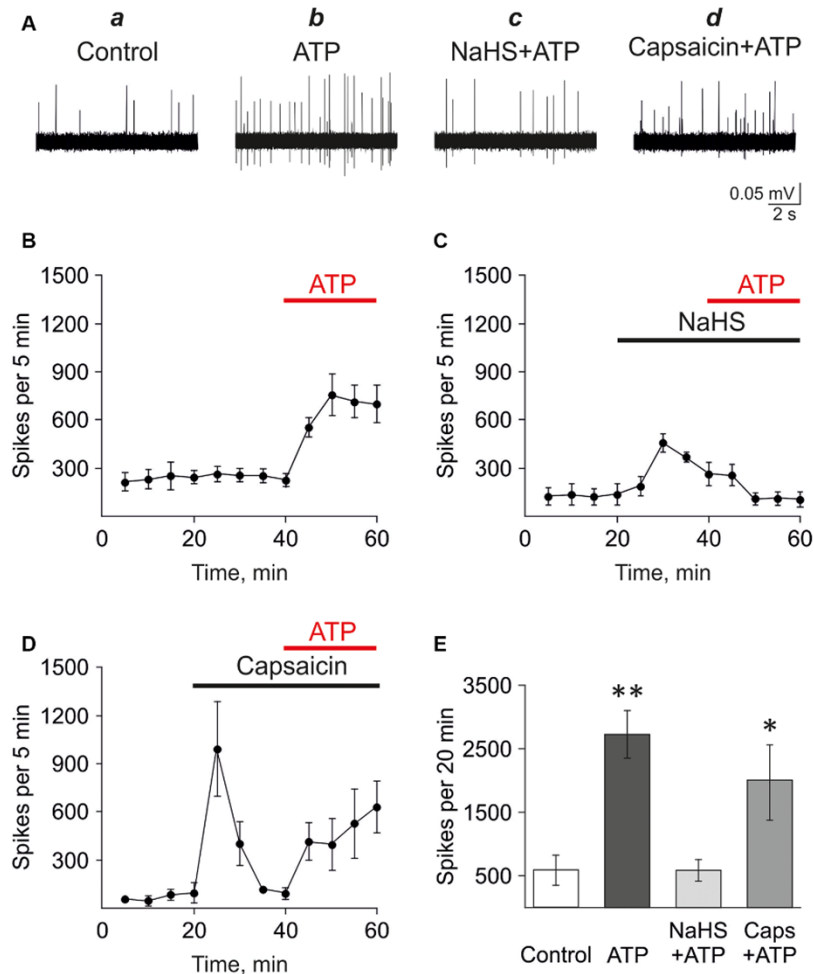- Interaction between H_2S and P2X receptors?

FIGURE 1 | Testing the action of hydrogen sulfide (H_2S) on the pro-nociceptive effect of ATP in trigeminal afferents. **(A)** Example traces of action potentials in the trigeminal nerve in control **(a)**, with ATP application (100 μM; **b**), ATP plus NaHS application after preincubation in NaHS (100 μM; **c**), ATP plus capsaicin application after preincubation in capsaicin (1 μM; **d**). **(B)** The frequency of action potentials during application of ATP ($n = 5$). **(C)** The frequency of action potentials during application of ATP (100 μM) in the presence of NaHS after preincubation with NaHS (100 μM; $n = 4$). **(D)** The frequency of action potentials during the application of ATP (100 μM) in the presence of capsaicin after preincubation with capsaicin (1 μM; $n = 4$). **(E)** The histograms showing the frequency of action potentials per 20 min in the trigeminal nerve in control and after application of ATP (100 μM), α,β-meATP (20 μM), in control and in the presence of NaHS or capsaicin. *$p < 0.05$, **$p < 0.01$.
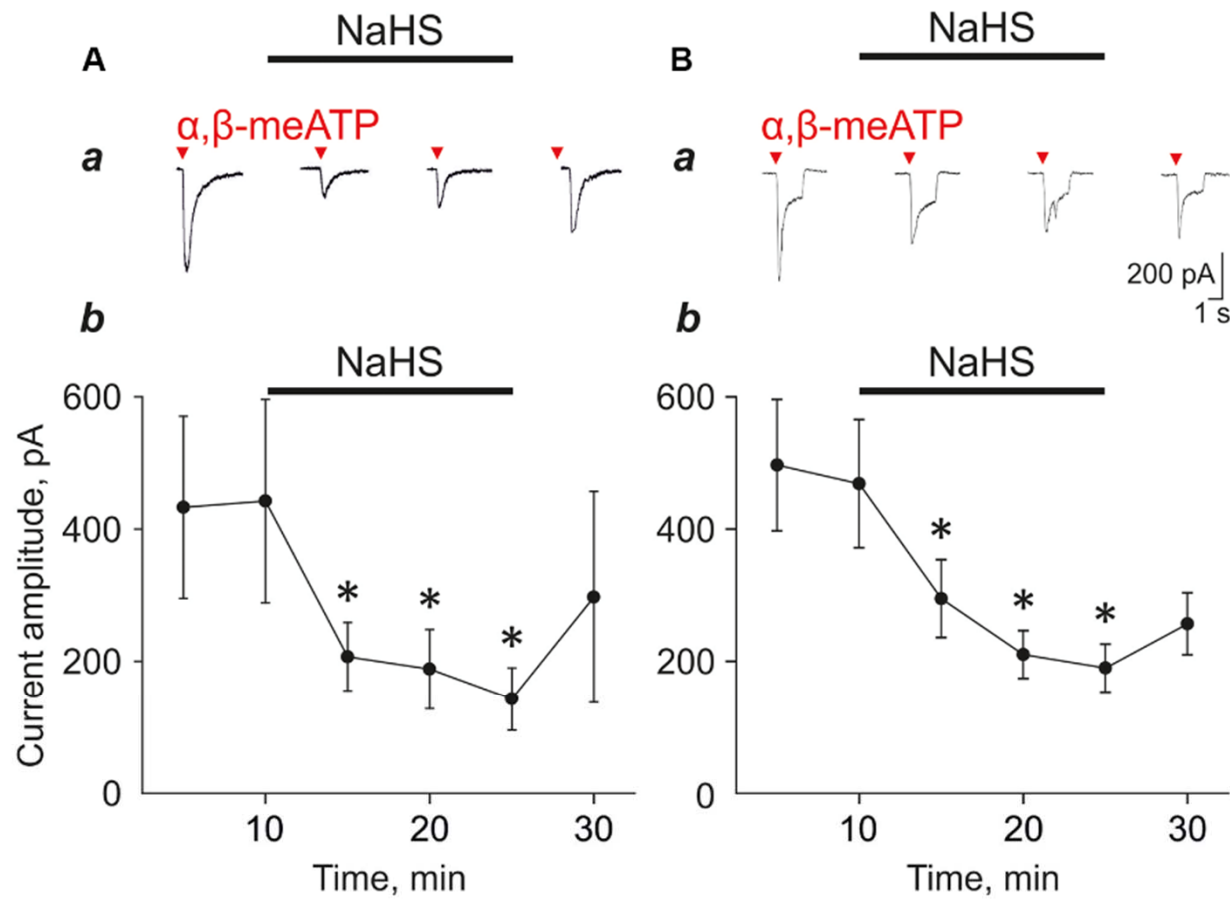
FIGURE 2 | Effect of NaHS (100 µM) on α,β-meATP induced currents in trigeminal ganglion neurons. **(A)** Examples of fast type currents in control and in the presence of NaHS **(a)**. Changes in the amplitude of the fast type currents (**b**, $n = 5$ cells). **(B)** Examples of mixed type currents in trigeminal ganglion neurons in control and in the presence of NaHS **(a)**. Changes in the amplitude of the fast component of the mixed type currents (**b**, $n = 9$ cells). *$p < 0.05$.
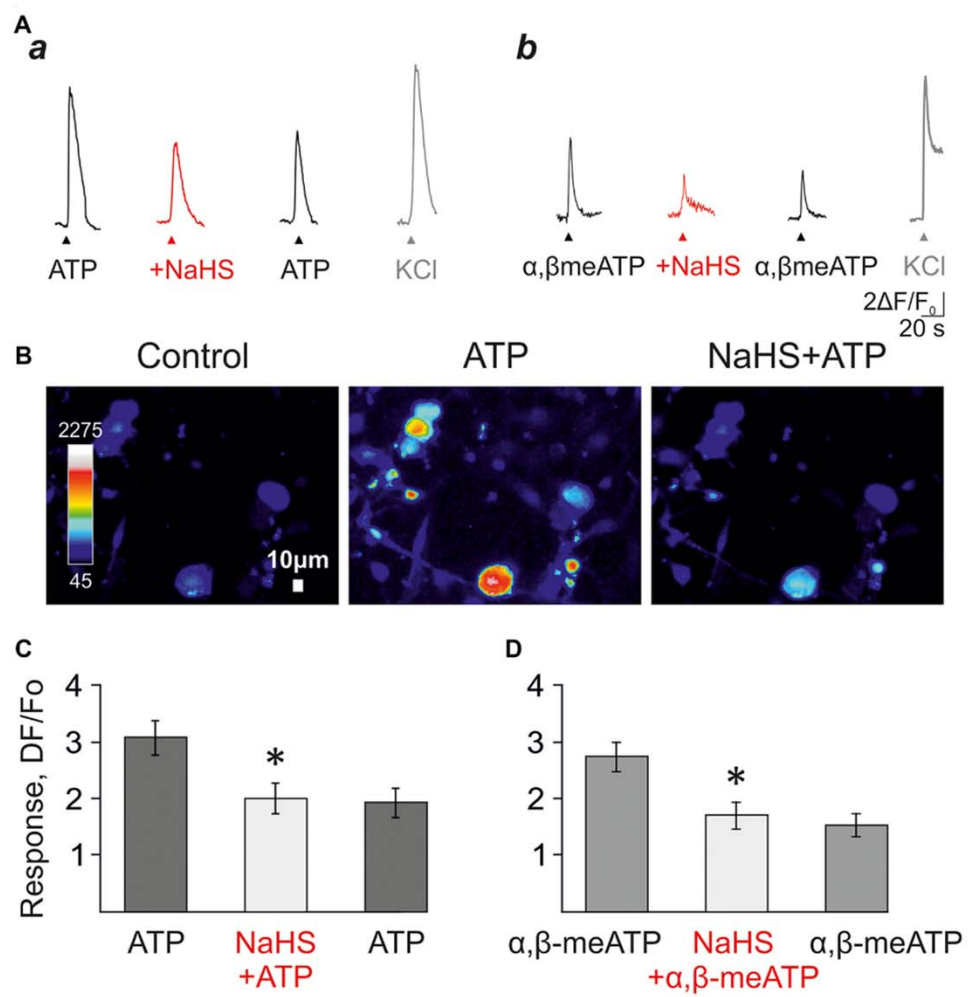
FIGURE 3 | The effect of NaHS on ATP-induced calcium signals in isolated trigeminal neurons. **(A)** Examples of calcium signals induced by application of 100 μM ATP **(a)**, or 20 μM α,β-meATP **(b)** in control, and in the presence of 100 μM NaHS. KCl was applied to distinguish neurons from trigeminal glial cells. **(B)** Pseudo-color images showing ATP-induced calcium signals in control and after the preliminary application of NaHS. **(C)** Histograms showing the amplitudes of calcium signals in response to the application of ATP (100 μM) in control, and in the presence of NaHS (n = 66 cells). **(D)** Histograms showing the amplitudes of calcium signals in response to applications of α,β-meATP (20 μM) in control, and in the presence of NaHS (n = 27 cells). *$p < 0.05$.
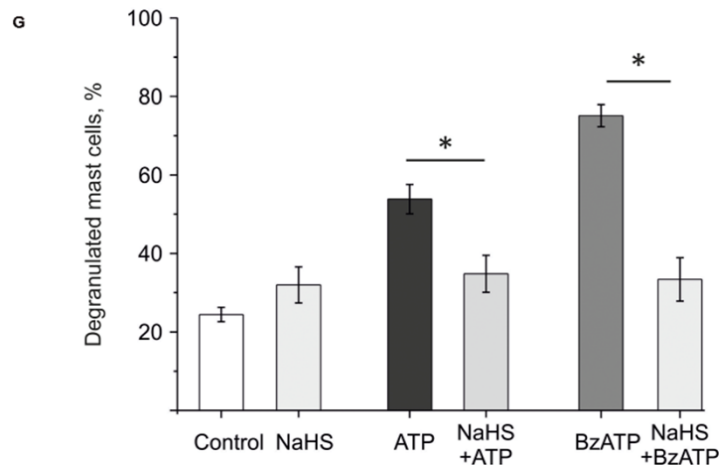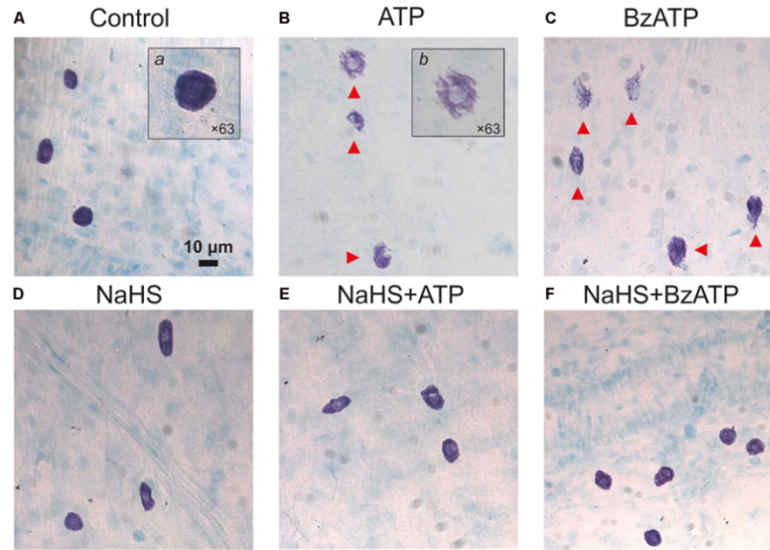
FIGURE 4 | Effect of the H$_2$S donor NaHS on ATP-induced mast cell degranulation. Images (×20) of Toluidin Blue stained rat meninges after incubation in basic solution **(A)** and after exposure to ATP (100 μM, **B**), BzATP (30 μM, **C**), NaHS (100 μM, **D**) or combination of NaHS+ATP **(E)** and NaHS+BzATP **(F)**. Notice red arrows indicating degranulated mast cells. Inserts **(a)** and **(b)** shows enlarged intact and degranulated mast cells (×63). **(G)** Histograms showing the percent of degranulated mast cells under various conditions ($n = 6$). *$p < 0.05$.
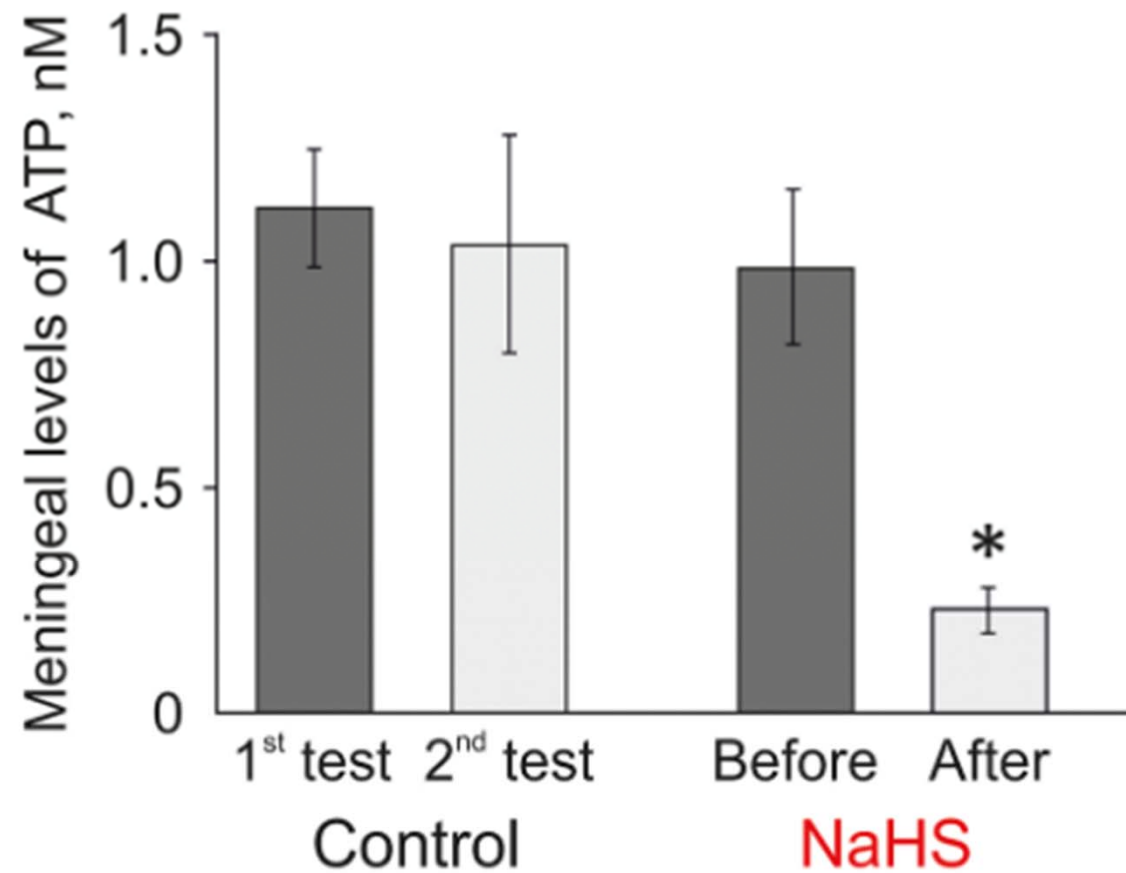
FIGURE 5 | Effect of the H$_2$S donor NaHS on the level of extracellular ATP in the meninges in a hemiskull preparation. The ATP level was twice determined in the basic solution in control (interval 20 min) or before and 20 min after incubation in 100 μM NaHS ($n = 8$). $^*p < 0.05$.

Conclusions

- In the meninges H2S has strong protective properties against nociceptive agent ATP

- H2S likely directly affects function of P2X receptors to prevent nociception

- H2S can be used as a treatment or prevention of migraines